

## A new concept for sensitive *in situ* stable isotope ratio infrared spectroscopy based on sample modulation

PETER WERLE\*†‡, CHRISTOPH DYROFF‡, ANDREAS ZAHN‡,  
PIERO MAZZINGHI† and FRANCESCO D'AMATO†

†CNR-National Institute for Applied Optics, Largo E. Fermi, 6, Florence, Italy

‡Institute for Meteorology and Climate Research, Research Center Karlsruhe, Germany

(Received 8 January 2005; in final form 6 April 2005)

Diode-laser absorption spectroscopy finds increasing applications in the emerging field of stable isotope research. To meet the requirements of the water isotopes measurement challenge in environmental research, ways have to be found to cope with the present limitations of spectroscopic systems. In this article, we discuss an approach based on the Stark effect in molecular spectra to reduce the influence of time-dependent, unwanted background structures generally superimposed on the desired signal from the spectral feature under investigation. A road map to high-sensitivity isotopic ratio measurements of water isotopes is presented. On the basis of an Allan Variance analysis of measured data, the detection limits have been calculated as a function of the integration time. To achieve the required optical density of about  $6 \times 10^{-7}$  for  $\text{H}_2^{17}\text{O}$  measurements, the duty cycle has to be optimized and the implementation of a sample modulation within an optical multipass cell is a promising approach to increase the stability of spectroscopic instrumentation required for ecosystem research and airborne atmospheric platforms.

**Keywords:** Diode-laser spectroscopy; Hydrogen-2; IR spectrometry; Isotope analysis; Oxygen-17; Oxygen-18; Sample modulation; Stark effect; Water

### 1. Introduction

Optical analytical techniques are well established not only in research laboratories, but also continue to find an increasing number of applications in industrial gas analysis and environmental sciences. A key issue in ecosystem research and atmospheric studies being conducted today is the ability to quantify small concentrations of trace gases [1]. Especially the *in situ* measurement of stable isotope ratios of stable molecular species (isotopomers) is still a challenge [2]. The measurement of isotopic ratios is a useful tool for studies in geochemistry, volcanology, biomedicine and atmospheric sciences. In environmental research, isotopic analysis provides information of the sources, sinks and transport of substances, and allows to estimate budgets of the major greenhouse gases, and several studies on atmospheric gases

---

\*Corresponding author. Tel.: +39-055-2308-405; Fax: +39-055-2337-409; Email: pwwerle@inoa.it

have been conducted [3]. The measurement of the isotopic composition of water vapour is an important issue [4]. Transport processes from the earth surface to the stratosphere are associated with a strong dehydration and due to isotopic fractionation, growing depletion in the stable isotopic ratios of water vapour can be observed with increasing height. A parameter, among others, which contributes to this effect is the speed of the lofting (cooling) process. Other shifts in the isotopic composition in the stratosphere are due to methane oxidation and chemical reactions with  $\text{HO}_x$  and  $\text{O}_x$  species. The importance of the isotope tracer to understand the transport and chemical processes in the free atmosphere has been recognized in the last few years [5]. Studies of the isentropic transport of water vapour into the lower stratosphere and the vertical transport into the tropopause region (extratropics) or the tropical transition layer (TTL) will contribute to an improved understanding of the water vapour budget in the upper troposphere and in the lower stratosphere (UT/LS) and will help to assess the potential change of water vapour and its impact to the earth's radiation budget and climate change. The German research ministry has recently approved the construction of a high-performance research aircraft. This High Altitude and LOng-range research aircraft (HALO) will be able to fly 8000 km before refueling – from Brazil to the South Atlantic, and from southeast Asia to arctic Russia [6]. The plane is designed to reach heights of up to 15,500 m and therefore allows to study the TTL and almost the entire lowermost stratosphere. The United States High-performance Instrumented Airborne Platform for Environmental Research (HIAPER), commissioned 3 years ago, is due to fly its first missions soon. Other airborne research platforms which are currently being used for atmospheric research are WB-57, ER-2 [7] and Geophysica [8]. To contribute to future missions of airborne platforms to understand the atmospheric water vapour budget as outlined above, the development of automated laser spectrometers for *in situ* measurements of D/H,  $^{17}\text{O}/^{16}\text{O}$  and  $^{18}\text{O}/^{16}\text{O}$  in  $\text{H}_2\text{O}$  is an important and challenging task [9].

Diode-laser systems have been developed for stable isotope ratio infrared (IR) spectroscopy of atmospheric gases as alternatives to conventional isotopic ratio mass spectrometers (IRMS) and have been applied to environmental measurements [9–21]. IRMS has high precision for  $\delta\text{D} \sim 1\text{‰}$ ,  $\delta^{18}\text{O} \sim 0.1\text{‰}$  and  $\delta^{17}\text{O} \sim 1\text{‰}$  but suffers from a poor temporal resolution. But this is required for ecosystem trace gas flux measurements [22, 23] and airborne applications, especially in the US time resolution causes a sampling and handling problem. Tunable diode-laser absorption spectroscopy provides the required temporal resolution but still is a technological challenge. Laser spectroscopy, in general, allows to distinguish between molecules with the same mass and does not require appropriate sample preparations such as purification, conversion and fragmentation.  $^{13}\text{CH}_4$  and  $^{12}\text{CH}_3\text{D}$ , which have nearly equal masses, are usually converted in to carbon dioxide and hydrogen for  $^{13}\text{C}/^{12}\text{C}$  and D/H measurements. Spectroscopic measurements allow non-destructive *in situ* measurements on a timescale of seconds and enable a compact design together with low power consumption. Therefore, this type of instruments is well suited for airborne applications.

The absorption spectrum has a characteristic fingerprint structure for each molecule and spectroscopic methods allow a highly specific detection of a broad range of substances. As it can be seen from figure 1, near-IR diode-lasers and mid-IR lead-salt diode-lasers as well as quantum cascade lasers cover the spectral range from the near- to the mid-IR and, therefore, can be used as versatile tunable laser sources for fast and highly sensitive spectroscopic trace gas analysis [24]. This measurement technique is based on absorption by the fundamental strong absorption bands of most gases in the mid-IR spectral region and by overtone and combination bands in the near-IR, where the oscillator strength is typically one to several orders of magnitude weaker than the IR-fundamental band. The most important application of diode-lasers is their use in conjunction with a long-path cell to provide high-sensitivity local measurements, when a single narrow laser line scans over an isolated absorption line of the species under investigation. Modulation techniques have made it possible to detect absorptions

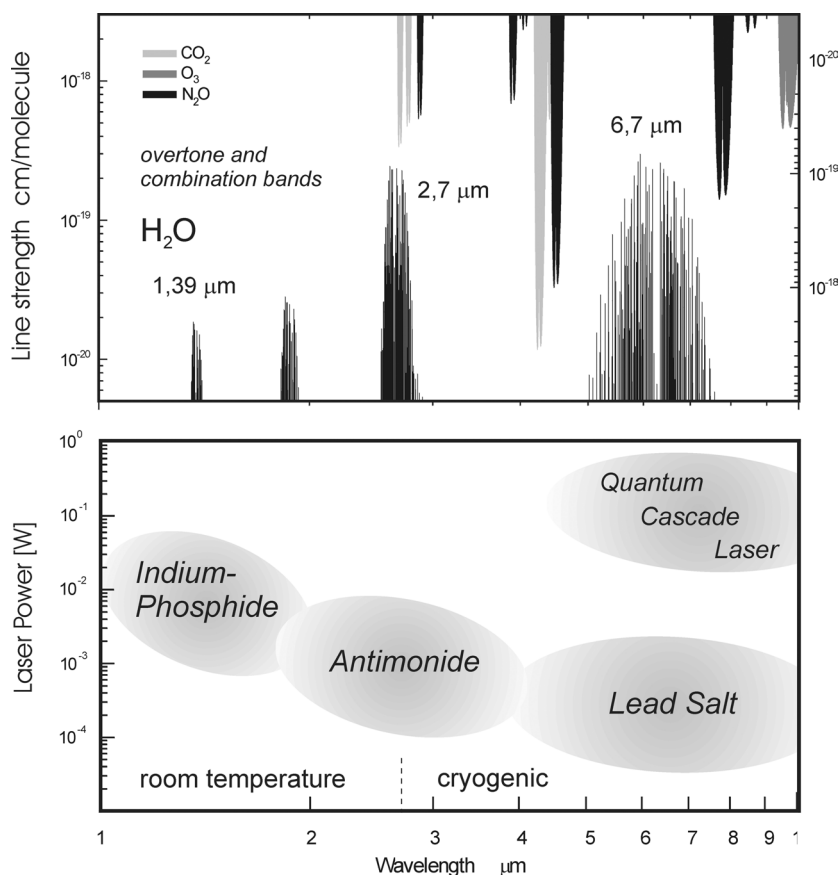


Figure 1. Overview plot: linestrength of combination, overtone and fundamental bands in the near- and mid-IR spectral region for water isotopes and interfering gases together with the available power from room temperature telecom and cryogenic lead-salt diode-lasers and quantum cascade lasers.

below  $10^{-6}$  for integration times of about 1 s [25]. This sensitivity, when combined with an optical path length through an absorbing sample of several tens of meters, translates into parts-per-billion (ppb) to parts-per-trillion (ppt) detections for many molecular species in the IR and for many gases with near-IR absorption bands, and this sensitivity corresponds to detection of sub-parts-per-million (ppm) concentrations over a path length of a few meters. When the wavelength of the diode-laser is tuned over an absorption line, a periodic, often non-stationary, fringe structure is superimposed to the desired signal from the absorption of the target gas, frequently called the 'etalon-effect'. These fringes are generated inside optical resonators in the path of the laser beam, built between surfaces of windows, lenses and even the laser and detector crystal. For spectroscopic techniques, the problem of fringe reduction is a key issue to improve sensitivity. An effective fringe reduction technique requires a selective modulation of the spectral feature under investigation without affecting fringes and background structure. The standard approach is to switch between ambient and background signals to suppress background fluctuations by subtracting them out [26]. This type of sample modulation is slow and especially for sticky, polar substances the exchange time can be long. It also reduces the duty cycle of the measurement often below 50 %. Therefore, a promising approach is the use of a fast sample modulation to separate disturbing background effects from the molecular feature of interest [27]. Laser Stark spectroscopy takes advantage of the fact that a given permanent

electric dipole moment of a molecule interacts with an external electric field. This interaction causes a shift of the energy levels and the line shape of the observed absorption transitions can be directly modulated through the application of an alternating field strength [28]. Although laser modulation is a prerequisite for low noise detection, the sample modulation is used to cope with time-dependent background structures and fringes. Besides water, other polar molecules suited for this type of sample modulation are, for example, formaldehyde, hydrogen peroxide, water, nitric acid, ammonia, hydrogen chloride, nitrogen dioxide and nitrous oxide.

## 2. Experimental details and results

The experimental setup for a sample modulation is shown in figure 2. A computer-controlled current ramp is superimposed to a DC-current offset to scan the diode-laser wavelength over a single absorption line with a repetition rate of 20 Hz. The absorption signal is detected after passing through the Stark absorption cell by a photovoltaic detector and amplified before it is processed in two steps with lock-in amplifiers. The first phase sensitive detection works at the laser modulation frequency,  $\omega_L$ , of 139 MHz [25] and generates a derivative-type signal as in conventional derivative spectroscopy. This technique provides a noise reduction and reduces the slope of the baseline. With a second lock-in amplifier that operates with the sample modulation frequency,  $\omega_S$ , as reference input, the sample modulation is detected and the signal is low-pass-filtered with a filter bandwidth of 125 Hz. Finally, the output signal is digitized and sent to a computer for further averaging and storage. Averaging of 64 individual scans led to an effective detection bandwidth of about 2 Hz. The data acquisition time for a concentration value was 3.2 s and the repetition rate was 6 s, because for an offline analysis all spectra have been transferred and stored. Usually, a part of the laser power is directed through

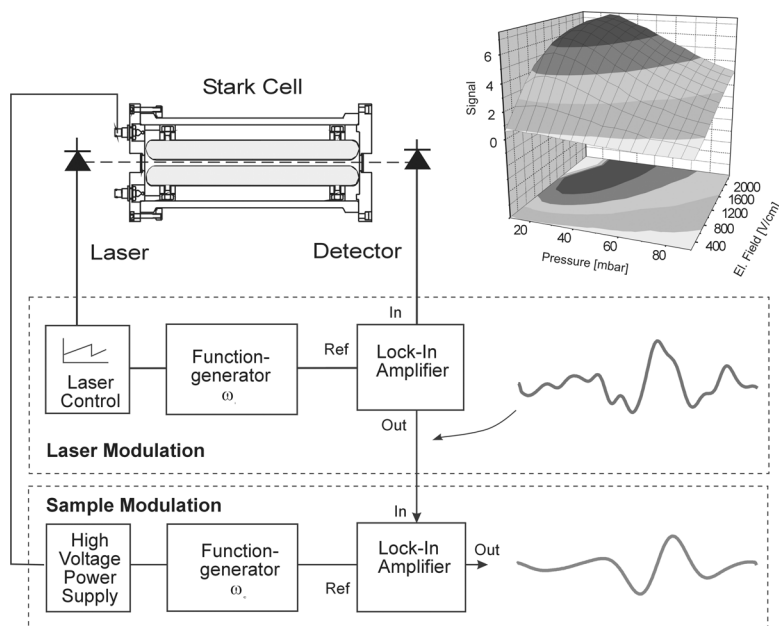


Figure 2. Schematic drawing of a diode-laser spectrometer for a sample modulation based on the Stark effect with the two subsequent lock-in amplifiers to record the signals from the laser and sample modulation. Also shown is the dependence of the output signal as function of the pressure and the electrical field in the Stark cell.

a reference cell on a second detector. This signal experiences no Stark sample modulation and is used for locking the diode-laser frequency to the observed absorption line, to compensate slow drifts in temperature and current of the diode-laser [26].

The sample is modulated in a special Stark absorption cell which has been designed to generate a strong electric field perpendicular to the laser beam. The Stark absorption cells contain stainless steel electrodes and the gap between the electrodes has been chosen to be 4.35 mm to obtain an optimum between the laser power passing through the gap and the electric field strength, and the optical single path inside the cell is 35 cm. The cell has at both ends BaF<sub>2</sub>-windows and 1/4 in. gas inlets and outlets. High voltage is introduced into the cell by vacuum-tight high-voltage plugs. The surface roughness was smoothed by polishing to avoid peaks of the electric field strength that give rise to electrical breakdown. But even for a perfectly uniform field distribution, there is a limitation for the applicable voltage, above which electrical breakdown occurs that is inevitable. The threshold voltage, which defines an upper limit for the generation of an electric field for a fixed electrode distance, can be calculated by the Paschen law [27]. The plot in figure 2 shows the calculated signal as a function of pressure inside the sample cell and the electrical field applied to the electrodes for Stark modulation. The pressure in the cell has to be low enough to avoid the pressure broadening of the absorption line yet should provide enough optical thickness for measuring low concentrations of trace gases. The stainless steel electrodes are connected to a high-voltage power supply (Burleigh, RC-45 CFT) which allows the generation of voltages up to 1 kV. The modulation amplitude was set well below the threshold voltage to avoid electrical breakdown.

To investigate the effect of a sample modulation, the Stark modulation has been applied to a constant concentration of formaldehyde from a calibration source [26], which is well suited for this investigation due to its strong electric dipole moment of 2.33 Debye comparable to water vapour, which has a dipole moment of 1.85 Debye. A sinusoidal high-voltage AC has been applied to the electrodes of the Stark absorption cell, whereas the same modulation signal was fed at the same time in the reference input of the lock-in amplifier, which was used for phase-sensitive detection of the Stark-modulated signal. The optimum signal for the observed absorption line doublet at 1757.94 cm<sup>-1</sup> could be achieved by a pressure in the cell of 25 mbar, a maximum Stark modulation amplitude of 2070 V/cm, limited by electrical breakdown, and a sample modulation frequency of  $\omega_S = 970$  Hz.

To compare measurements with and without sample modulation, time series data have been recorded. The measurements for both techniques have been done in the same manner. First, the absorption cell was flushed with zero air to record possibly appearing background structures, which are subtracted from the current ambient air spectra. Then a constant flow of 1 l/min (STP) air through the cell has been established. During all measurements, the cell pressure has been actively stabilized to 25 mbar. The mixing ratio of formaldehyde was adjusted to an optical depth of  $4.1 \times 10^{-4}$  for the 35 cm single path length. With this constant gas flow, first a calibration spectrum has been recorded, to which the relative concentration of 1.0 has been assigned. Subsequent sample spectra have been recorded with the same volume mixing ratio with a repetition rate of 6 s and an effective bandwidth of 2 Hz. A fitting algorithm based on a multiple linear regression analysis [26] calculated the time series concentration data.

The signal without sample modulation as shown in the upper part of figure 2 has superimposed a periodic fringe structure. In contrast, the sample-modulated signal is very smooth, indicating no symptom of interfering étalon fringes. The comparison of the measurements is illustrated in figure 3a and b, where time series data for both techniques are shown. The system stability according to the calculated time series concentration values has been characterized by the Allan variance [29]. If we plot the Allan variance as a function of the averaging time, we get at the minimum of the Allan variance the optimum averaging time, which is a characteristic for a given instrument, in our case for a given measurement method. Figure 3a

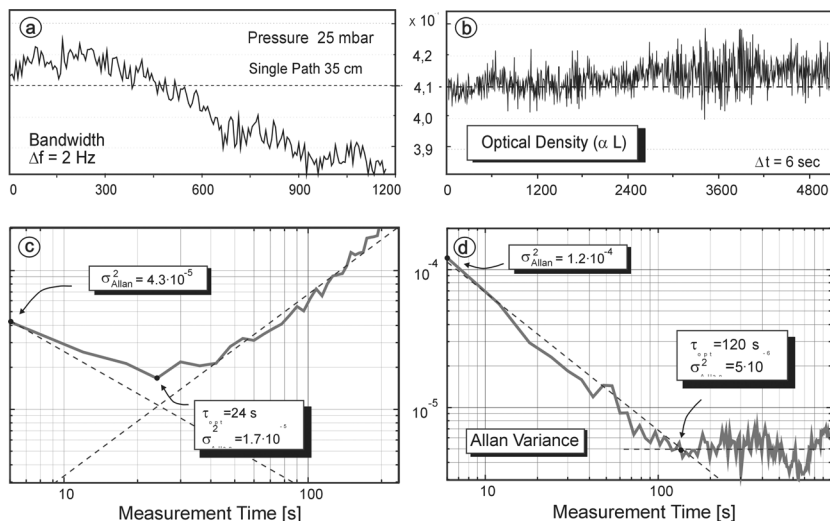


Figure 3. Allan Variance analysis of time series data from measurements with the sample modulation (a) off and (b) on. The corresponding Allan plots show that (c) without sample modulation drift effects start to dominate after about 24 s, whereas (d) with the Stark modulation no drift effects occur.

shows the measurement without sample modulation, which indicates a significant decline of the recorded time series data of the relative sample concentration, although a constant value ( $=1.0$ ) would have been expected. This strong drift has been caused by the presence of fluctuating background structures such as a moving fringe. The negative influence of this signal drift finds its equivalent in the corresponding Allan plot shown in figure 3c. Up to 24 s signal averaging leads to a linear decrease of the Allan variance, with the minimum value of  $1.7 \times 10^{-5}$ . Beyond this optimum integration time, the Allan variance, and with it the instrument's detection limit, will deteriorate as a consequence of disturbing background drifts. It should be emphasized that the minimum of the Allan variance indicates that the optimum integration interval within both background spectrum and ambient air spectrum recording has to be completed [29]. For recording of the ambient air spectrum, only less than half of the overall integration time is available due to the required gas exchange times. In contrast, the relative concentration recorded with the sample modulation technique exhibits almost no deviation from the expected constant value. Only slight increment in the noise of the relative concentration values can be noticed. The calculated Allan variance in figure 3d illustrates this behaviour. Starting with a higher value than in the sample unmodulated case, the Allan variance declines linearly with the integration time, reflecting a white-noise-dominated region. The sample modulation technique yields an optimum integration time of 120 s which is five times the optimum integration time required without modulation. Strongly correlated with this enhanced integration time is a notable gain in the Allan variance by a factor of more than  $3 \times 10^{-6}$  to a value of  $5 \times 10^{-6}$ . For integration times beyond 120 s, the Allan plot shows a horizontal level, which indicates the presence of  $1/f$ -type noise [29]. Further averaging will not help to improve the detection limit. Probably this  $1/f$ -type noise will be caused by the turbulent gas flow through the absorption cell which is strongly related to refractive index fluctuations [31]. Without sample modulation, half of the time is lost by recording background spectra, but there is no need for background measurement by the sample modulation technique. So, the whole integration time is available for measurement, doubling thereby the duty cycle of the system. The price we have to pay for this is that the initial Allan variance at 6 s is higher for the double modulation scheme, equivalent to the slightly higher noise in the

time series data. In the sample modulation case, we detect the difference in the signals with the electrical field on and off and therefore we always lose some amplitude as the signal does not completely disappear under modulation. The lock-in amplifier measures a smaller signal voltage, which then reduces the signal-to-noise and, therefore, increases the noise in the time series data. However, due to the increased stability this initial loss can easily be compensated and for longer integration times higher sensitivity can be obtained.

The Allan variance analysis is very convenient for the predictions of sensitivities as a function of integration time [29]. All measurements were performed at an optical density  $(\alpha L) = 4.1 \times 10^{-4}$  at a 35 cm single path length. The detection limit can easily be calculated by multiplying the initial optical density by the square root of the Allan variance for a given measurement time. Without sample modulation, we obtain for 6 s an optical density of  $(\alpha L)_{\min} = 2.7 \times 10^{-6}$  ( $\Delta f = 2$  Hz) and for the optimum integration time of 24 s we obtain  $(\alpha L)_{\min} = 1.7 \times 10^{-6}$ . For the sample modulation technique, we obtain for 6 s an optical density of  $(\alpha L)_{\min} = 4.5 \times 10^{-6}$  and for the optimum integration time of 120 s we obtain  $(\alpha L)_{\min} = 9 \times 10^{-7}$ . All these numbers are calculated from data measured at a time interval of 6 s and, therefore, concentrations and detection limits up to the maximum integration time can be calculated. Any extrapolation beyond the optimum integration time determined for the given experimental conditions leads to meaningless numbers, as the relationship between the sample and background spectra is lost [29].

### 3. Discussion of performance and requirements

Typical ambient concentrations for atmospheric water vapour are listed in table 1 for altitudes of 9 and 13 km. For a required precision of  $\delta D = 30\%$ ,  $\delta^{18}\text{O} = 10\%$  and  $\delta^{17}\text{O} = 10\%$ , we obtain the required detection limits as shown in table 2. Using the mid-IR lines of Webster and Heyms field near  $6.7 \mu\text{m}$  [7] and the near-IR lines of Kerstel *et al.* around  $1.39 \mu\text{m}$  [10], we obtain for an altitude of 13 km in the near- and mid-IR for the required optical density values for  $\text{H}_2^{16}\text{O}$ ,  $\text{H}_2^{16}\text{O}$ ,  $\text{H}_2^{16}\text{O}$  and HDO as listed in table 3 from the 2004 edition of the HITRAN database [30]. For  $\text{H}_2^{17}\text{O}$ , we have the strongest requirements for the minimum optical density and we calculated for a pathlength  $L = 56$  m, a pressure in the sample cell of  $p = 25$  hPa and a temperature  $T = 323$  K a value of  $(\alpha L)_{\min} = 5.95 \times 10^{-7}$  at  $1484.5 \text{ cm}^{-1}$  and a substantially lower value in the near-IR. If we compare this requirement with the measurements presented above, it is obvious that a multipass cell has to be applied and the duty cycle of the measurement has to be improved to provide a faster data sampling rate for airborne measurements. The duty

Table 1. Ambient conditions and concentrations for atmospheric water isotopes for altitudes of 9 and 13 km.

Altitude (km)	$p$ (hpa)	$T$ (K)	$[\text{H}_2\text{O}]$ (ppmv)	$[\text{H}_2^{18}\text{O}]$ (ppbv)	$[\text{H}_2^{17}\text{O}]$ (ppbv)	[HDO]
9	307	230	50	85.2	17.6	4.7
13	165	215	10	17	3.5	0.93

Table 2. Required detection limits derived from the required measurement precision of  $\delta D = 30\%$ ,  $\delta^{18}\text{O} = 10\%$  and  $\delta^{17}\text{O} = 10\%$  for altitudes of 9 and 13 km.

Altitude (km)	$p$ (hpa)	$T$ (K)	$[\text{H}_2\text{O}]$ (ppbv)	$[\text{H}_2^{18}\text{O}]$ (pptv)	$[\text{H}_2^{17}\text{O}]$ (ppbv)	[HDO] (pptv)
9	50	323	500	852	176	140
13	50	323	100	170	35	28

Table 3. Calculated minimum optical densities for water isotopes based on the required minimum detectable concentrations at an altitude of 13 km.

Isotope	Wavenumber (cm <sup>-1</sup> )	Integration line strength (cm <sup>2</sup> cm <sup>-1</sup> atm <sup>-1</sup> ) (natural abundance)	[c] <sub>min</sub> (ppb) at 13 km	Minimum optical density at L = 56 m, p = 25 hPa, T = 323 K,	Sensitivity gain NIR→MIR
H <sub>2</sub> <sup>16</sup> O	7183.6858	3.671E-24	100	4.35E-8	16
	1484.25726	1.78E-23		6.97E-7	
H <sub>2</sub> <sup>18</sup> O	7183.58578	6.33E-24	0.170	4.15E-8	64
	1483.92607	8.39E-23		2.66E-6	
H <sub>2</sub> <sup>17</sup> O	7183.73545	1.194E-24	0.035	1.46E-8	40
	1484.51094	1.97E-23		5.95E-7	
HDO	7183.97279	3.385E-25	0.028	3.63E-9	195
	1484.10644	2.32E-23		7.08E-7	

cycle issue is not critical as even for the given data acquisition a 100 % duty cycle can be easily obtained by simply not storing all spectra. Then a value for  $(\alpha L)_{\min} = 9 \times 10^{-7}$  could be measured within 60 s instead of 120 s. For practical reasons and a field usable system especially onboard of an aircraft, a higher dynamic reserve is desirable for the signal-to-noise ratio to provide reliable data. Therefore, we calculated the expected improvement when going from a 35 cm single pass to a 56 m multipass cell, which provides a potential improvement by a factor of 160. In this case, we should be able in principle to obtain a value of  $(\alpha L)_{\min} = 2.8 \times 10^{-8}$  for 3.2 s time resolution. Even if we assume that we might lose a factor of 10 due to laser power losses after multiple reflections, we still should reach a value of  $(\alpha L)_{\min} = 2.8 \times 10^{-7}$  for 3.2 s, which in turn would exceed the requirement value of  $(\alpha L)_{\min} = 5.95 \times 10^{-7}$ . Figure 4 summarizes all this in a road map to high-sensitivity isotopic ratio measurements of water isotopes. On the basis of Allan Variance analysis of measured data, the detection limits have been calculated as a function of the integration time (figure 4a) with and without (figure 4b) sample modulation. To reach the required minimum optical density of about  $6 \times 10^{-7}$  for

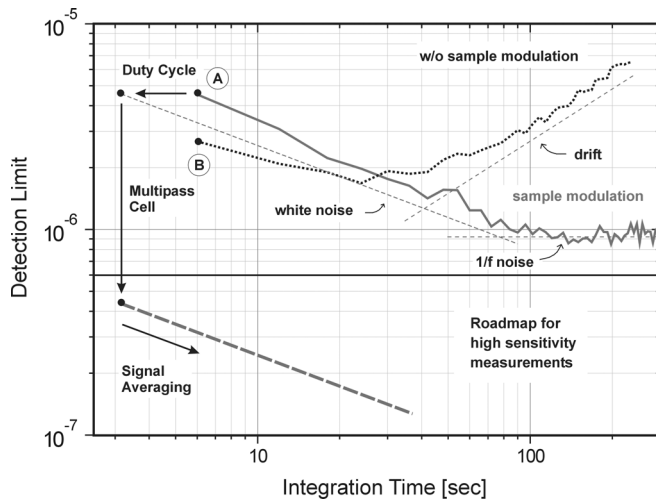


Figure 4. Detection limits as a function of the integration time derived from the Allan Variance analysis (a) with and (b) without sample modulation. The arrows show that in order to reach a required value of  $6 \times 10^{-7}$ , starting from (a) the duty cycle has to be optimized and a multipass cell has to be used together with digital signal averaging. Also plotted is the theoretical dependence of white noise, 1/f-noise and linear drift as a function of integration time.

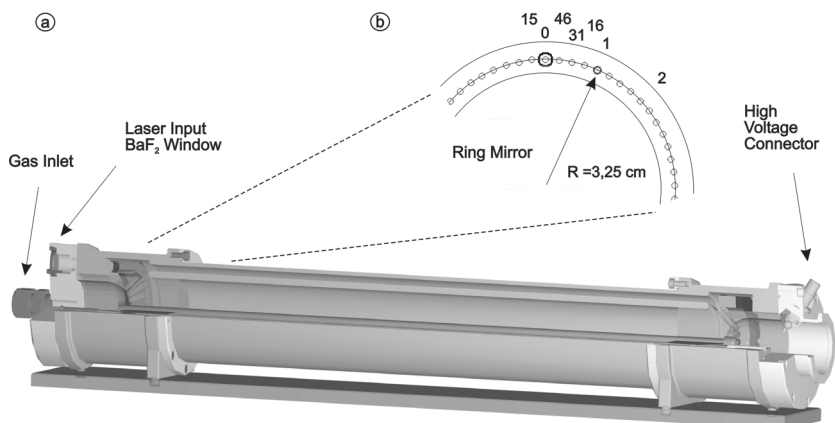


Figure 5. Layout of the multipass Stark sample modulation cell. The laser enters the cell through a BaF<sub>2</sub> window on the left side and passes between the high-voltage electrodes, which have the form of two coaxial cylinders separated by 5 mm. The ring mirror has 61 spots distributed on a radius of 3.25 cm, which leads to an optical path length of 56 m and an active volume of 500 ml for the cell.

H<sub>2</sub><sup>17</sup>O, the duty cycle should be optimized and a multipass cell has to be used. For a 56 m multipass cell, the scale factor with respect to the 35 cm single pass would be 160, but for extrapolations we only applied a factor of 10. Further improvement can be achieved by digital signal averaging, if no technical noise limits the performance.

In principle, the multipass approach may work without sample modulation, but at these low optical densities usually fringes and drifts dominate the system performance even more and it is a worthwhile task to have a sample modulation implemented to cope with these problems. Therefore, based on the single pass experiments and the operational parameters found there, a prototype multipass cell for Stark modulation with an optical pathlength of 56 m has been designed and built as displayed in figure 5. The laser beam enters through a 5 mm hole in a ring mirror and then rotates on 61 spots at a radius of 32.5 mm around the centre of the cell as displayed in figure 5b. The radius of curvature of the ring mirrors is  $R = 11$  m and the mirrors are separated by 46 cm. After 122 passes, the beam exits at the entry hole. The electrodes have the form of two coaxial cylinders and the inner and outer electrodes are separated by 5 mm. Special care has been taken to avoid a turbulent gas flow through the cell, which might lead to disturbances during the measurement [31]. Two ceramic insulators guide the gas flow between the electrodes and also back to the cell exit again. The overall volume of the cell is less than half a litre and therefore allows a rapid gas exchange and a fast response to concentration changes. Detailed measurements are underway to investigate the cell characteristics before an implementation in an airborne system starts.

#### 4. Summary and conclusions

The problem of baseline drifts is the key issue for the design of ultra-sensitive spectrometers as well as for operational instrumentation for field measurements. Several approaches towards the quantum limit use clever designs and measurement techniques [32–35], but they do not fully solve the problem of baseline drift. The application of an additional sample modulation such as the Stark effect is an efficient method for the suppression of background fluctuations. We demonstrated a substantial improvement of the system stability and useful integration

times, which is a prerequisite for improving the detection limits and/or measurement precision. Moreover, because of the lack of interfering background structures, there is no need for background recording and subtraction and this technique will provide enhanced duty cycles. This is important, because most polar, sticky molecules require long exchange times with zero air in the sample cell [26]. This type of sample modulation technique is applicable to all molecules with a permanent dipole moment such as water vapour, formaldehyde, hydrogen peroxide, nitric acid, ammonia, hydrogen chloride, nitrogen dioxide and nitrous oxide.

With a 35 cm single pass setup, a value for  $(\alpha L)_{\min} = 9 \times 10^{-7}$  within 120 s has been measured. The duty cycle of about 50 % can be increased to 100 %, which in turn will lead to an improvement by approximately a factor of 2 giving a detection limit of  $4.5 \times 10^{-7}$  (see ref. [29] for a detailed treatment of dead time and duty cycle). Alternatively, the measurement speed can be improved. The integration time during the sample modulation was limited to about 120 s due to the presence of  $1/f$ -type noise in the system (*i.e.* a constant level of the Allan Variance at longer integration times), which can be attributed either to the presence of spurious side modes during laser operation and/or to the presence of turbulence effects in the single pass cell. It is important to mention that even for longer integration times no significant drift influence (*i.e.* an increase in the Allan Variance at longer integration times) can be observed when the sample modulation has been used. For real field and airborne measurement applications, of course a long path cell has to be applied and, therefore, a 56 m multipass cell suitable for Stark sample modulation has been developed. The principal gain factor of 160 when increasing the optical path from 35 cm to 56 m can be used – at least in part – to improve signal-to-noise ratio, sensitivity and detection speed by proper adjustment of the operating conditions and, therefore, we think that according to this roadmap we will be able to deliver high-quality measurements of water vapour isotopes and other trace gases in the future.

## References

- [1] P. Werle. Diode-laser sensors for *in situ* gas analysis. In *Lasers in Environmental and Life Sciences—Modern Analytical Methods*, P. Hering, P. Lay and S. Stry (Eds), chapter 11, pp. 223–243, Springer Verlag, Heidelberg (2004); and references therein.
- [2] E. Kerstel. Isotope ratio infrared spectrometry. In *Handbook of Stable Isotope Analytical Techniques*, P.A. de Groot (Ed.), chapter 34, pp. 759–787, Elsevier, Amsterdam (2004); and references therein.
- [3] D. Ehhalt, M. Prather, F. Dentener, R. Derwent, E. Dlugokencky, E. Holland, I. Isaksen, J. Katima, V. Kirchhoff, P. Matson, P. Midgley, M. Wang. IPCC 2001: Atmospheric chemistry and greenhouse gases. In *Climate Change 2001: The Scientific Basis. Contribution of Working Group I to the Third Assessment Report of the Intergovernmental Panel on Climate Change*, J.T. Houghton, Y. Ding, D.J. Griggs, M. Noguer, P.J. van der Linden, X. Dai, K. Maskell and C.A. Johnson (Eds), p. 881, Cambridge University Press, Cambridge/New York (2001).
- [4] K.H. Rosenlof. How water enters the stratosphere. *Science*, **302**, 1691–1692 (2003).
- [5] A. Zahn. Constraints on 2-way transport across the Arctic tropopause based on O<sub>3</sub>, stratospheric tracer SF<sub>6</sub> ages, and water vapor isotope (D, T) tracers. *J. Atmos. Chem.*, **39**, 303–325 (2001).
- [6] Q. Schirnmeier. Research plane will scale uncharted heights. *Nature*, **431**, 390 (2004).
- [7] C. Webster, A.J. Heymsfield, Water isotope ratios D/H, <sup>18</sup>O/<sup>16</sup>O, <sup>17</sup>O/<sup>16</sup>O in and out of clouds map dehydration pathways. *Science*, **302**, 1742–1747 (2003).
- [8] M. Pantani, F. Castagnoli, F. D’Amato, M. De Rosa, P. Mazzinghi, P. Werle. Two infrared laser spectrometers for the *in situ* measurement of stratospheric gas concentration. *Infrared Phys. Tech.*, **46**, 109–113 (2004).
- [9] E.R.T. Kerstel, R. van Trigst, N. Dam, J. Reuss, H.A.J. Meijer. Simultaneous determination of the <sup>2</sup>H/<sup>1</sup>H, <sup>17</sup>O/<sup>16</sup>O, and <sup>18</sup>O/<sup>16</sup>O isotope abundance ratios in water by means of laser spectroscopy. *Anal. Chem.*, **71**, 5297–5303 (1999).
- [10] E.R.T. Kerstel, G. Gagliardi, L. Gianfrani, H.A.J. Meijer, R. van Trigst, R. Ramaker. Determination of the D/H, <sup>17</sup>O/<sup>16</sup>O, and <sup>18</sup>O/<sup>16</sup>O isotope ratios in water by means of tuneable diode-laser spectroscopy at 1.39 μm. *Spectrochim. Acta A*, **58**, 2389–2396 (2002).
- [11] L. Gianfrani, G. Gagliardi, M. van Burgel, E.R.T. Kerstel. Isotope analysis of water by means of near infrared dual-wavelength diode-laser spectroscopy. *Opt. Express*, **11**, 1566–1576 (2003).
- [12] P. Bergamaschi, G.W. Harris. Measurements of stable isotope ratios (<sup>13</sup>CH<sub>4</sub>/<sup>12</sup>CH<sub>4</sub>; <sup>12</sup>CH<sub>3</sub>D/<sup>12</sup>CH<sub>4</sub>) in landfill methane using a tunable diode-laser absorption spectrometer. *Global Biogeochem. Cy.*, **9**, 439–447 (1995).

- [13] P. Bergamaschi, C.A.M. Brenninkmeijer, M. Hahn, T. Rockmann, D.H. Scharffe, P.J. Crutzen, N.F. Elansky, I.B. Belikov, N.B.A. Trivett, D.E.J. Worthy. Isotope analysis based source identification for atmospheric CH<sub>4</sub> and CO sampled across Russia using the trans-Siberian railroad. *J. Geophys. Res.*, **103**, 8227–8235 (1998).
- [14] A.A. Kosterev, R.F. Curl, F.K. Tittel, C. Gmachl, F. Capasso, D.L. Sivco, J.N. Baillargeon, A.L. Hutchinson, A.Y. Cho. Methane concentration and isotopic composition measurement with a mid-infrared quantum-cascade laser. *Opt. Lett.*, **24**, 1762–1764 (1999).
- [15] C.R. Webster, G.J. Flesh, D.C. Scott, J.E. Swanson, R.D. May, W.S. Woodward, C. Gmachl, F. Capasso, D.L. Sivco, J.N. Baillargeon, A.L. Hutchinson, A.Y. Cho. Quantum cascade laser measurements of stratospheric methane and nitrous oxide. *Appl. Opt.*, **40**, 321–326 (2001).
- [16] M. Erdélyi, D. Richter, F.K. Tittel. <sup>13</sup>CO<sub>2</sub>/<sup>12</sup>CO<sub>2</sub> isotopic ratio measurements using a difference frequency-based sensor operating at 4.35 μm. *Appl. Phys. B*, **75**, 289–295 (2002).
- [17] J.B. McManus, M.S. Zahniser, D.D. Nelson, L.R. Williams, C.E. Kolb. Infrared laser spectrometer with balanced absorption for measurement of isotopic ratios of carbon gases. *Spectrochim. Acta A*, **58**, 2465–2479 (2002).
- [18] R. van Trig, H.A.J. Meijer, A.E. Sveinbjornsdottir, S.J. Johnsen, E.R.T. Kerstel. Measuring stable isotopes of hydrogen and oxygen in ice: the bølling transition in the dye-3 (south Greenland) ice core. *Ann. Glaciol.*, **35**, 125–130 (2002).
- [19] K. Yamamoto, N. Yoshida. High-precision isotopic ratio measurement system for methane (<sup>12</sup>CH<sub>3</sub>D/<sup>12</sup>CH<sub>4</sub>, <sup>13</sup>CH<sub>4</sub>/<sup>12</sup>CH<sub>4</sub>) by using near-infrared diode laser absorption spectroscopy. *Spectrochim. Acta A*, **58**, 2699–2707 (2002).
- [20] G. Gagliardi, A. Castrillo, R.Q. Iannone, E.R.T. Kerstel, L. Gianfrani. High-precision determination of the <sup>13</sup>CO<sub>2</sub>/<sup>12</sup>CO<sub>2</sub> isotope ratio using a portable 2.008 μm diode-laser spectrometer. *Appl. Phys. B*, **77**, 119–124 (2003).
- [21] K. Uehara, K. Yamamoto, T. Kikugawa, N. Yoshida. Site-selective nitrogen isotopic ratio measurement of nitrous oxide using 2–5 μm diode lasers. *Spectrochim. Acta A*, **59**, 957–962 (2003).
- [22] D.R. Bowling, S.D. Sargent, B.D. Tanner, J.R. Ehleringer. Tunable diode laser absorption spectroscopy for stable isotope studies of ecosystem-atmosphere CO<sub>2</sub> exchange. *Agr. Forest Meteorol.*, **118**, 1–19 (2003).
- [23] T.J. Griffis, J.M. Baker, S.D. Sargent, B.D. Tanner, J. Zhang. Measuring field-scale isotopic CO<sub>2</sub> fluxes with tunable diode-laser absorption spectroscopy and micrometeorological techniques. *Agr. Forest Meteorol.*, **124**, 15–29 (2004).
- [24] P. Werle, F. Slemr, K. Maurer, R. Kormann, R. Mücke, B. Jänker. Near- and mid-infrared laser-optical sensors for gas analysis. *Opt. Lasers Eng.*, **37**, 101–114 (2002).
- [25] P. Werle. A review of recent advances in semiconductor laser based gas monitors. *Spectrochim. Acta A*, **54**, 197–236 (1998).
- [26] P. Werle, P. Mazzinghi, F. D’Amato, M. De Rosa, K. Maurer, F. Slemr. Signal processing and calibration procedures for *in situ* diode-laser absorption spectroscopy. *Spectrochim. Acta A*, **60**, 1685–1705 (2004).
- [27] P. Werle, S. Lechner. Stark-modulation-enhanced FM-spectroscopy. *Spectrochim. Acta A*, **55**, 1941–1955 (1999).
- [28] G. Herzberg. *Molecular Spectra and Molecular Structure*. Van Nostrand Reinhold Company, New York (1950).
- [29] P. Werle, R. Mücke, F. Slemr. Limits of signal averaging in atmospheric trace gas monitoring by tuneable diode-laser absorption spectroscopy. *Appl. Phys. B*, **57**, 131–139 (1993).
- [30] L.S. Rothman, R.R. Gamache, R.H. Tipping, C.P. Rinsland, M.A.H. Smith, D.C. Brenner, V. Malathy Devi, J.M. Flaud, C. Camy-Peyret, A. Perrin, A. Goldman, S.T. Massie, L.R. Brown, R.A. Toth. HITRAN molecular database. *J. Quant. Spectrosc. Ra.*, **48**, 469–507 (1992).
- [31] P. Werle, B. Jänker. High frequency modulation spectroscopy: phase noise and refractive index fluctuations in optical multipass cells. *Opt. Eng.*, **35**, 2051–2057 (1996).
- [32] J. Ye, L.S. Ma, J.L. Hall. Ultrasensitive detections in atomic and molecular physics: demonstration in molecular overtone spectroscopy. *J. Opt. Soc. Am. B*, **15**, 6–14 (1997).
- [33] E.R. Crosson, K.N. Ricci, B.A. Richman, F.C. Chilese, T.G. Owano, R.A. Provencal, M.W. Todd, J. Glasser, A.A. Kachanov, B.A. Paldus, T.G. Spence, R.N. Zare. Stable isotope ratios using cavity ring-down spectroscopy: determination of <sup>13</sup>C/<sup>12</sup>C for carbon dioxide in human breath. *Anal. Chem.*, **74**, 2003–2007 (2002).
- [34] J. Morville, D. Romanini, M. Chenevier. Patent WO03031949, Universite J. Fourier, Grenoble, France (2003).
- [35] A. Castrillo, G. Casa, M. van Burgel, D. Tedesco, L. Gianfrani. First field determinations of the <sup>13</sup>C/<sup>12</sup>C isotope ratio in volcanic CO<sub>2</sub> by diode-laser spectrometry. *Opt. Express*, **304**, 6515–6523 (2004).